Ultra-fast Fiber Bragg Grating Inscription in CYTOP Polymer Optical Fibers using Phase Mask and 400 nm Femtosecond Laser

YING-GANG NAN,[1]* DAMIEN KINET,[1] KARIMA CHAH,[1] IVAN CHAPALO[1], CHRISTOPHE CAUCHETEUR[1], AND PATRICE MÉGRET[1]

[1]*Electromagnetism and Telecommunication Department, Université de Mons, 31 Boulevard Dolez, Mons, 7000, Belgium*
[*]*Yinggang.NAN@umons.ac.be*

Abstract: Fiber Bragg gratings (FBGs) in cyclic transparent fluoropolymer (CYTOP) optical fiber are the subject of a lot of research as they can be of interest for many applications, such as temperature, humidity, strain, and radiation sensing. We report here a new technique to produce high quality FBGs in CYTOP fiber. It uses a femtosecond laser system operating at 400 nm and a phase mask. In contrast to previously reported results, the gratings are obtained in a few seconds with a writing power as low as 80 µW. With this setup, 2 mm-long gratings with reflectivity up to 92 % and full width at half maximum bandwidth around 0.5 nm were obtained in less than 10 s. The resonance wavelengths of the FBGs are confirmed by numerical computation in the graded-index multimode CYTOP fiber, and the mode selection characteristic of FBGs in CYTOP is investigated. Finally, the temperature sensitivity of CYTOP FBG is measured in different mode groups for heating up and cooling down, showing values independent of the mode group measured, but with a small hysteresis.

1. Introduction

With the continued development of optical fibers in the field of communication and sensing, multimode polymer optical fibers (POF) have attracted more and more attention due to their advantages such as large fiber parameters, low Young's modulus, and high bandwidth [1–4]. According to the shape of the refractive index distribution in the fiber, multimode fibers (MMF) are classified as step-index fibers or graded-index fibers. However, in multimode step-index fibers, the eigenmodes have in general different propagation delays, resulting in pulse broadening [5–7], that limits the transmission rates. To solve this shortcoming, graded-index fibers are an essential solution, for which the index profile is designed such that all the eigenmodes have nearly the same running time.

The first commercial graded-index polymer fiber was based on methyl methacrylate (PMMA) and manufactured by Kwangju Institute of Science and Technology (KIST) from South Korea in 2000. Its attenuation was as high as 210 dB/km at 652 nm [8], and it was caused by the high absorption of the C−H bonds present in the fiber [9, 10]. To solve this problem, hydrogen atoms were replaced by heavy fluorine atoms, which results in a cyclic transparent optical polymer (CYTOP) giving the best results in producing low attenuation polymer optical fibers. Subsequently, it became obvious to consider combining the CYTOP with Bragg grating for sensing applications [11–15].

To date, two main ways have been successfully demonstrated to inscribe fiber Bragg grating (FBG) in CYTOP POF. Firstly, the FBG is directly inscribed in CYTOP using a plane-by-plane method and a femtosecond laser at 517 nm with a pulse energy of 80 nJ [16, 17]. The high laser energy allows the FBG to be inscribed in the CYTOP fiber without removing the over-cladding. However, the over-clad of the CYTOP could be damaged to some extent due to the high energy

exposure needed during the inscription. This damage will destroy the structure of the fiber and result in distortion of the FBG spectrum. Moreover, this setup requires an accurate control of the beam spot position and the high precision motion stage for the fiber displacement, and is time-consuming as well. Comparing with the phase mask technique, the main shortcoming of the plane-by-plane writing method is the low repeatability during the FBG inscription.

Another main method to fabricate FBG in CYTOP is using Krypton fluoride (KrF) excimer laser at 248 nm with the phase mask technique [18–20]. In this method, the over-cladding of the CYTOP should be removed before irradiation, which results in an easy inscription, even at low beam energy. However, this method produces FBG with low reflectivity, many unidentified peaks, and is time-consuming, e.g., 60 min, 42 min, and 30 min, respectively in [18], [19] and [20]. Thus, it is essential to find new methods to keep a balance between the quality and efficiency in the process of fabricating FBG in CYTOP.

In this work, we combine a phase mask technique with a femtosecond laser system operating at 400 nm to inscribe FBG in CYTOP fiber with reflectivity at 1550 nm up to 92 % in less than 10 s exposure time. The working wavelength of the CYTOP FBG is chosen in the third telecommunication window (1) to be compatible with existing silica-based FBGs, and (2) to use classical low cost measuring equipment. The main advantage of the proposed method is the use of standard precision mechanical equipment to inscribe highly reflective CYTOP FBGs in a fast and repeatable way. To demonstrate the quality of the gratings, the locations of the peak resonance wavelengths are calculated in CYTOP fiber by numerical computations, and are correlated with the experimental ones. Then the temperature sensitivity of the different mode groups of FBGs in CYTOP is investigated to show that these FBGs can be used as temperature sensors, even if they are multimoded.

2. Bragg grating fabrication

2.1. POF Pretreatment

We use the commercially available graded-index (GI) multimode perfluorinated POF (GigaPOF-50SR from Chromis), with an over-clad diameter, a core diameter and a numerical aperture of 490 µm, 50 µm and 0.185, respectively [21]. We experimentally notice that over-clad made of polycarbonate (PC) material has a lower fs-laser radiation damage threshold than the core of the fiber. In other words, the over-clad is more easily damaged compared with the core for the same beam power exposure. From our experiments, we found that the maximum threshold power of the over-clad is around 300 µW, which is significantly lower than the core threshold power of 10 mW for a 5 mm-long grating as shown in Fig. 1 (a).

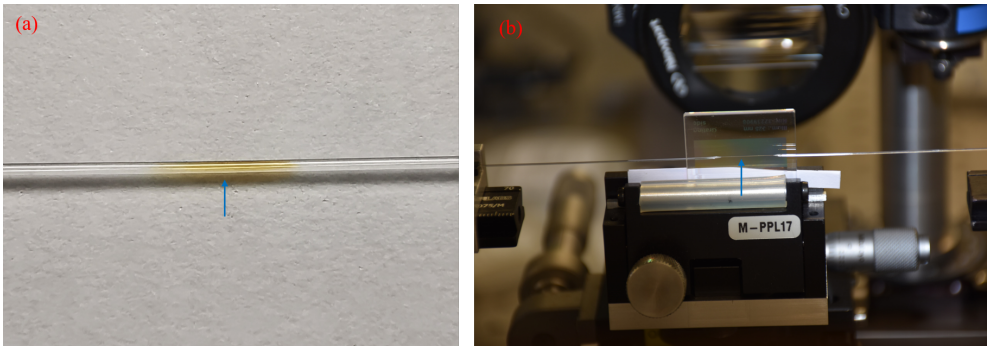

Fig. 1. (a) Yellow brown damage of the CYTOP with over-clad due to beam power exceeding 300 µW for a 5 mm-long grating; (b) CYTOP fiber without over-clad.

Moreover, because the phase mask technique is used, two requirements are necessary: (1) the fiber should be positioned close to the phase mask, and (2) enough energy radiation is necessary to inscribe a FBG in the fiber core. Therefore, to inscribe a FBG in large diameter fibers using the phase mask technique, the second requirement plays the main role in this experiment. As a consequence, there is a high risk to damage the over-clad as well as the phase mask during the inscription process with the over-clad. To avoid these drawbacks and to inscribe a high quality FBG, 2-cm long polycarbonate over-clad is removed by dichloromethane CH_2Cl_2 in 10 min [22–25]. This is shown in Fig. 1 (b), where the trickiest part of this removal process is the cleaning of the PC residues that could affect the geometry of the core interface. Indeed, any residues will distort the inscription pattern, and lead to huge distortions of the grating spectrum.

2.2. Experimental set-up

Figure 2 represents the experimental setup used to write the gratings. It consists of a femtosecond laser (Spitfire Pro amplifier from Spectra Physics company) producing 120 fs light pulses at 800 nm with a repetition rate of 1 kHz and energy of 4 mJ. The laser is followed by a variable attenuator and a frequency doubler to have pulses at 400 nm. The laser beam diameter is then reduced by a diaphragm to 2 mm, and focused onto the core of the CYTOP fiber through the phase mask by a plano-convex cylindrical lens with a focal length of 100 mm. The phase mask has a period of 1158 nm, and a powermeter is inserted between the lens and the diaphragm to measure the power of the beam.

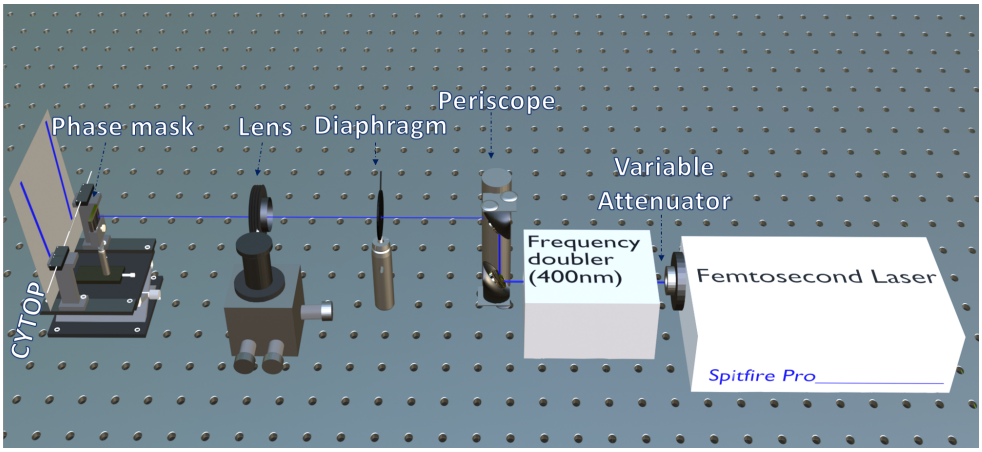

Fig. 2. Experimental setup to inscribe FBG in CYTOP fiber.

An FBG interrogator (FS2200 from FiberSensing) with a spectral resolution of 1 pm and a spectral range from 1500 nm to 1600 nm is used to monitor FBG spectrum evolution in real-time. A butt coupling between a standard single-mode silica optical fiber pigtail (SMF-28) and the CYTOP fiber is used as a link towards the interrogator. A small drop of refractive index matching gel (n = 1.4646 at 589.3 nm) is used between the two optical fibers to reduce Fresnel reflections from the interfaces of the SMF and CYTOP.

2.3. FBG spectrum in CYTOP

The length of the grating is starting at 2 mm in this work. Figure 3 shows the spectra for a 2 mm-long grating (#1) inscribed in 10 s with a beam power as low as 80 µW. From the transmission spectrum, the reflectivity of the grating #1 is calculated to be 92 %. Nevertheless, it should be noted that the reflectivity values calculated using the transmission spectrum should

be considered rather as estimation than precise values, mainly because the connection of the MMF and SMF forms a multimode - single-mode structure that leads to the presence of an interferometric signal in the transmission spectrum that complicates the reference level estimation when calculating the reflectivity. Taking this factor into account, we estimate the reflectivity of the FBGs from the absolute power values of the reflection peaks that are recorded using the same connection method and interrogator.

To investigate the FBG spectral responses to the different beam powers, we inscribe several FBGs with the same grating length and different exposure powers, as depicted in Fig. 4 for three 2 mm-long gratings using a beam power of 80 µW, 100 µW and 120 µW, respectively. Comparing these spectra, it shows that (1) the main resonance peak decreases with the increase of the beam power, (2) the maximum power of the peak is approximately −10 dBm for the lowest beam power equal to 80 µW, and (3) there are more and more subpeaks when the beam power is increased. It is also important to note that for beam powers lower than 80 µW, there is no resonance peak in the spectrum.

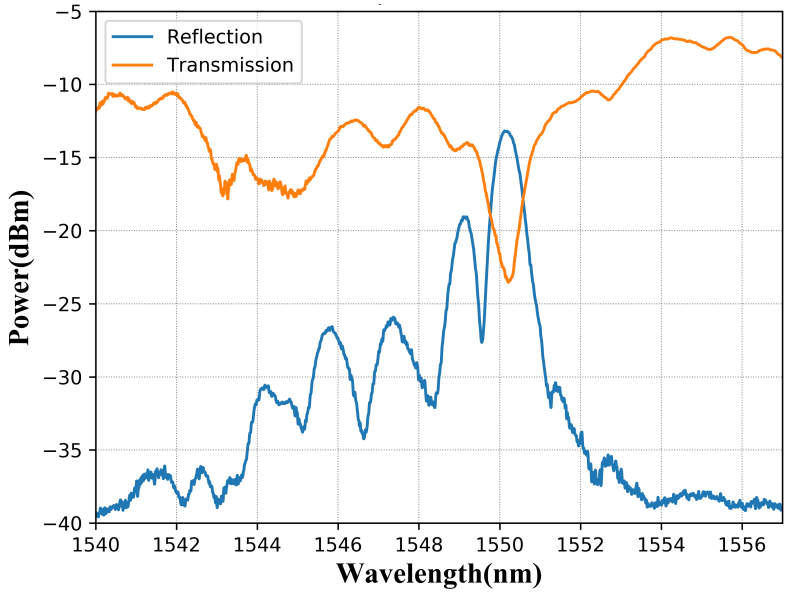

Fig. 3. Transmission and reflection spectra for grating #1 (inscription parameters: grating length 2 mm, laser power 80 µW, and inscription time 10 s).

From this series of experiments, it is concluded that the most suitable beam power is 80 µW for a 2 mm-long grating in CYTOP without over-clad based on a femtosecond laser system operating at 400 nm and using a phase mask technique.

To probe further, we have produced gratings of different lengths by adjusting the diameter of the diaphragm in Fig. 2. Increasing the diaphragm diameter increases the grating length, but it also increases the power reaching the core of the fiber. Figure 5 shows the FBG spectra for different grating lengths. It shows that (1) the power of the main peak increases with the increase of the grating length, (2) the maximum peak power is −7 dBm for a 5 mm-long grating inscribed with a beam power equal to 110 µW, and (3) all the spectra exhibit significant subpeaks compared with Fig. 4.

During each inscription process, the distance between phase mask and CYTOP is kept constant, therefore the height of the main peak of the spectra mainly depends on two parameters: the beam power and the grating length. The relation between these two parameters is shown in Fig. 6: the

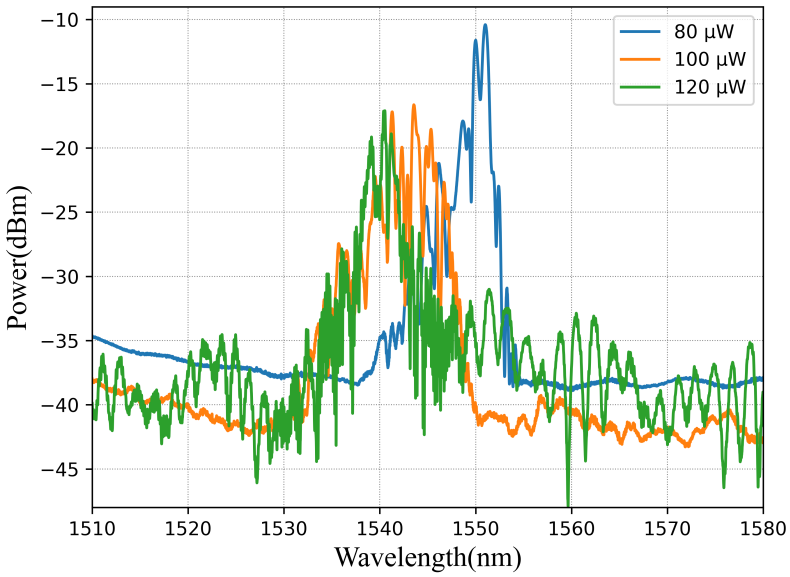

Fig. 4. Reflection spectra for three gratings: #2 (inscription parameters: grating length 2 mm, laser power 80 µW, and inscription time 10 s); #3 (inscription parameters: grating length 2 mm, laser power 100 µW, and inscription time 9 s); #4 (inscription parameters: grating length 2 mm, laser power 120 µW, and inscription time 7 s).

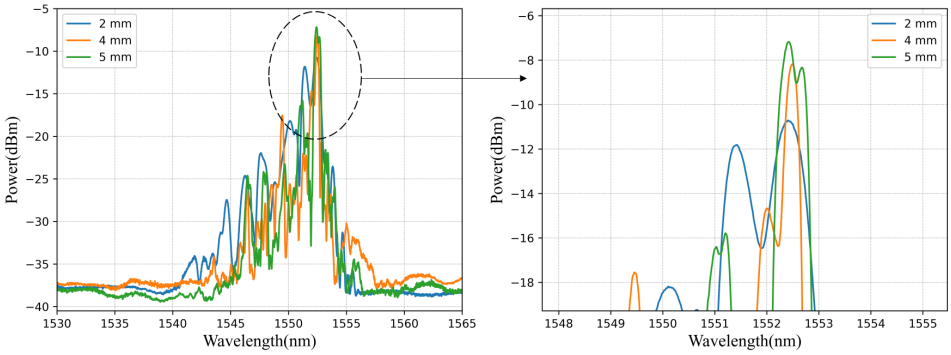

Fig. 5. Reflection spectra for different grating length: #2 (inscription parameters: grating length 2 mm, laser power 80 µW, and inscription time 10 s); #5 (inscription parameters: grating length 4 mm, laser power 100 µW, and inscription time 16 s); #6 (inscription parameters: grating length 5 mm, laser power 110 µW, and inscription time 30 s).

power of the spectra decreases when beam power exceeds a suitable threshold. Moreover, the power of the spectra increases with the increase of the grating length when the average beam power is maintained at the same level at the surface of the fiber. The best inscription beam powers for CYTOP fiber without over-clad are approximately 80 µW, 100 µW and 110 µW for grating length of 2 mm, 4 mm and 5 mm, respectively. In the following section, the characteristics of the FBG spectrum and the mode selection in CYTOP fiber are investigated.

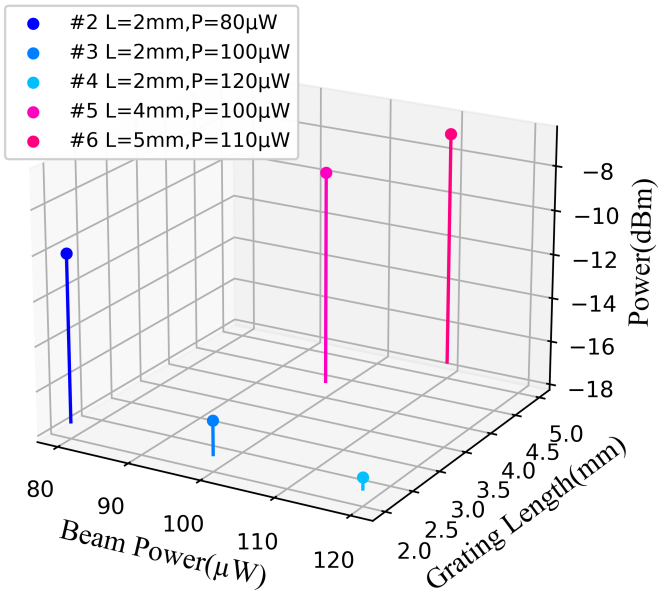

Fig. 6. The evolution of the peak power under different inscription conditions.

3. Mode Selection

Currently available CYTOP POF are multimode fibers. Therefore FBGs in this type of fibers are multimoded, and mode selection naturally occurs in the experimental setup as it mixes polymer multimode fibers with silica singlemode fibers. Going back to the multimode fiber theory, it is possible to explain the resonance locations found in the experimental spectra.

A graded index fiber is characterized by the core radius a and the refractive indices of the core n_{co} and the cladding n_{cl} or, alternatively, by the numerical aperture NA. For parabolic graded-index multimode fibers, the refractive index profile is given by

$$n^2(r) = \begin{cases} n_{\mathrm{co}}^2 \left(1 - 2\Delta \frac{r^2}{a^2}\right) & 0 < r < a \\ n_{\mathrm{cl}}^2 & r \geq a \end{cases} \tag{1}$$

where $n(0) = n_{\mathrm{co}}$, $n(a) = n_{\mathrm{cl}}$, and $\Delta = \frac{n_{\mathrm{co}}^2 - n_{\mathrm{cl}}^2}{2n_{\mathrm{co}}^2}$ is the index difference between core and cladding. Besides, another important parameter is the normalized frequency V, defined as

$$V = \frac{2\pi a \mathrm{NA}}{\lambda} \tag{2}$$

where

$$\mathrm{NA} = \sqrt{n_{\mathrm{co}}^2 - n_{\mathrm{cl}}^2} = n_{\mathrm{co}}\sqrt{2\Delta} \tag{3}$$

is the numerical aperture of the fiber.

For a parabolic graded-index fiber, the estimated number N of modes that can propagate is given by [26]

$$N = \frac{V^2}{4} \tag{4}$$

and can therefore be significant when V is large. For example, the number of modes of our CYTOP fiber is more than 80 at 1550 nm. Whereas there are many possible modes, they can be clustered in groups of modes having nearly the same propagation constant (β), and for parabolic graded index profile, the approximate number M of such mode groups is given by [27, 28]

$$M = \sqrt{N} = \frac{V}{2} \tag{5}$$

For the CYTOP fibers used in our setup, NA $\approx$ 0.185, $n_{\mathrm{co}} \approx 1.342$, $a = 25\,\mu$m, leading to $V \simeq 18.7$ and $M \simeq 9$ for λ around 1550 nm.

The effective refractive index n_m of the m^{th} mode group can be expressed as [29, 30]

$$n_m = n_{\mathrm{co}}\sqrt{1 - 4m\Delta/\mathrm{V}} \tag{6}$$

where $m = 1, 2, 3, ..., M$. Following reference [30], the cross-mode parameter describes a mode excited by the two neighbouring mode groups m and $m+1$. From the Bragg wavelength equation $\lambda_{\mathrm{Bragg}} = 2n_{\mathrm{eff}}\Lambda$, we can calculate the resonance wavelength of the m^{th} mode group and m^{th} cross-mode group by the following equations

$$\lambda_m = 2n_m\Lambda \tag{7a}$$

$$\lambda_m^{\mathrm{cross}} = (n_m + n_{m+1})\Lambda \tag{7b}$$

where the period of grating is $\Lambda = 579$ nm in this simulation. Using Eq. 6, Eq. 7a and Eq. 7b, the wavelength spacing between two adjacent mode groups reflection peaks is given by [30]

$$\Delta\lambda = \frac{\lambda_0^2 \mathrm{NA}}{2\pi a n_{\mathrm{co}}^2} \tag{8}$$

The wavelength spacing between two adjacent mode groups reflection peaks is equal to 1.57 nm in CYTOP fiber.

Table 1. The distribution of Bragg resonance wavelengths in CYTOP fiber

m	n_m	λ_m (nm)	$\lambda_m^{\mathrm{cross}}$ (nm)
1	1.3406	1552.48	1551.68
2	1.3392	1550.89	1550.10
3	1.3379	1549.31	1548.52
4	1.3365	1547.73	1546.94
5	1.3351	1546.14	1545.35
6	1.3338	1544.56	1543.76
7	1.3324	1542.97	1542.17
8	1.3310	1541.38	1540.58
9	1.3296	1539.78	

Table 1 shows the resonance wavelengths of the m^{th} mode group and m^{th} neighboring cross-mode group, and these values are compared in Fig. 7 with an experimental spectrum of a

5 mm-long grating inscribed at 110 µW. The black dotted lines and red dotted lines represent the resonance wavelength locations of the mode group and the cross-mode group, respectively. It is clearly seen that the agreement between the experimental spectra and the computed resonance wavelengths is quite good. The experimental wavelength spacing between reflection peaks corresponding to adjacent mode groups is equal to 1.50 nm that is close to the computation value of 1.57 nm.

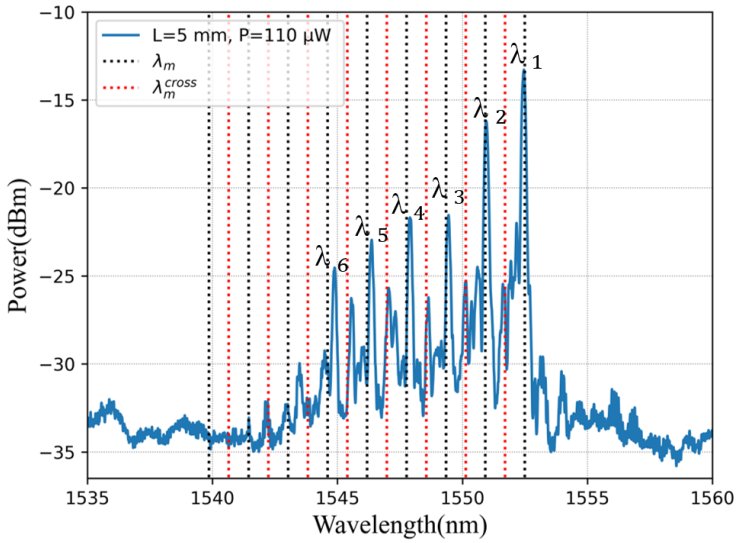

Fig. 7. Comparison between the FBG resonance wavelengths of Eqs. (7) and the experimental FBG spectrum: #7 (inscription parameters: grating length 5 mm, laser power 110 µW, and inscription time 30 s).

The reflection spectrum measurement depends on the power distribution among the different mode groups, that, in turn, depends on the mode selection of the SMF in this SMF-CYTOP configuration. Therefore, changing the coupling conditions between the CYTOP and SMF achieves a mode selection as shown in Fig. 8.

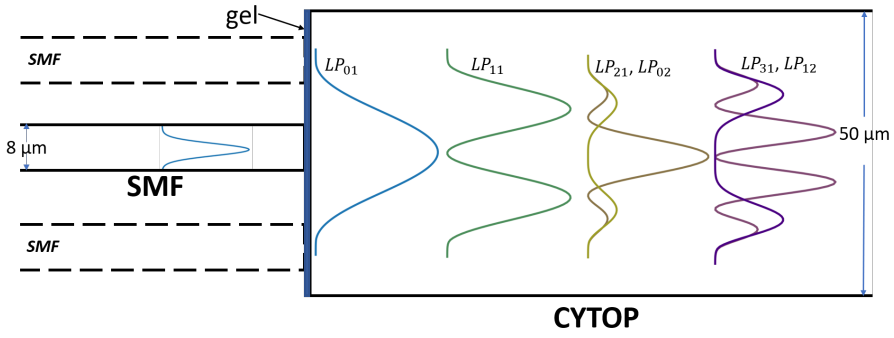

Fig. 8. Experimental layout of fiber connection between SMF and CYTOP fiber.

To demonstrate this mode selection, Figure 9 shows the spectrum of the different mode groups when the coupling conditions between the SMF and the CYTOP fiber are varied. It is clearly

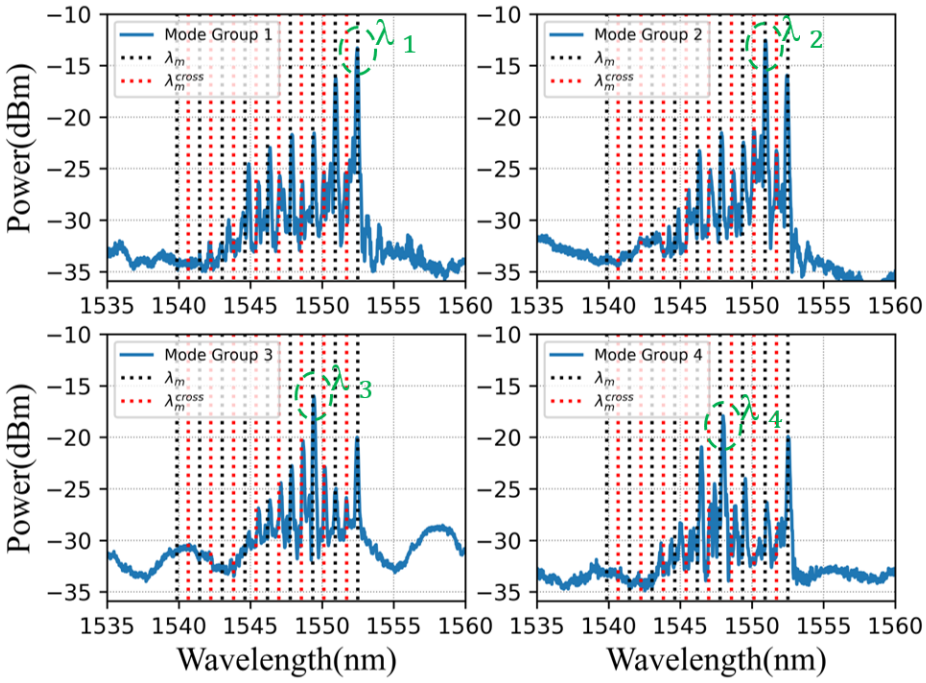

Fig. 9. Spectrum of the mode groups in CYTOP for grating #7 when launching conditions are varied.

seen that the different mode groups can be excited just by changing the coupling conditions. The wavelength locations of the mode groups have again a good agreement with the computed results under different mode selection conditions. Moreover, the appearance of the cross-modes depends on whether the neighboring mode groups will be excited. This mode selection ability has great scalability and can be applied to other working, such as mode-selective fiber Bragg grating laser.

4. Temperature measurements

To characterize the sensing properties of the inscribed gratings in CYTOP fibers, we investigate their temperature sensitivities in different mode groups. It is well-known that the Bragg wavelength shifts with changes of temperature is described by the relation [31]:

$$\frac{\Delta\lambda_{\text{Bragg}}}{\lambda_{\text{Bragg}}} = (\alpha + \xi)\Delta\text{T} \tag{9}$$

where α is the thermal expansion coefficient, and ξ is the thermo-optic coefficient. For pure silica, the thermal expansion coefficient is 0.55×10^{-6}/°C and the thermo-optic coefficient is equal to 8.3×10^{-6}/°C [32]. The temperature sensitivity of pure silica is thus 13.66 pm/°C at 1543 nm, and is dominated by the thermo-optic coefficient as it is 15 times higher than the thermal expansion coefficient. For a grating in a silica-based fiber, the temperature sensitivity is equal to 10.37 pm/°C at 1543 nm [33].

In polymers, however, the thermal expansion coefficient is usually positive and the thermo-optic coefficient is negative [19]. From the literature [20, 34], it is found that the thermal expansion coefficient and the thermo-optic coefficient of CYTOP material are equal to 7.4×10^{-5}/°C and -5.0×10^{-5}/°C, respectively. This leads to a temperature sensitivity of CYTOP FBGs of

37 pm/°C at 1550 nm, that is thus approximately 3 times higher than for silica.

To date, some articles give the temperature sensitivity of the first mode group of FBGs in CYTOP fibers without over-clad and fabricated by KrF excimer laser at 248 nm. Zheng *et al.* [20] reported a temperature sensitivity equal to 27.5 ± 2.4 pm/°C in the temperature range 20 °C to 55 °C, whereas Koerdt *et al.* obtained 23 to 26 pm/°C in the range 10 °C to 30 °C, respectively [19]. However, there are no detail articles that report and investigate the temperature sensitivity of the different mode groups in CYTOP-FBGs.

To measure the temperature sensitivity of the different mode groups of the FBGs in CYTOP fiber, a climate chamber (Weiss SB 22 [35]) is used to control the temperature and humidity during the experiment with a temperature range of −40 °C to 180 °C and a relative humidity range of 10 % to 98 %. Considering the maximum temperature tolerance of CYTOP fiber (<70 °C), we cycle the temperatures from 10 °C to 60 °C with steps of 5 °C (heating up) and −5 °C (cooling down), and the humidity is kept approximately constant around 80 %. The time to make two full temperature cycles is approximately 20 h, and the FBG spectrum is recorded 10 min after setting up each step. Figure 10 shows the temperature response of a 5 mm-long inscribed at

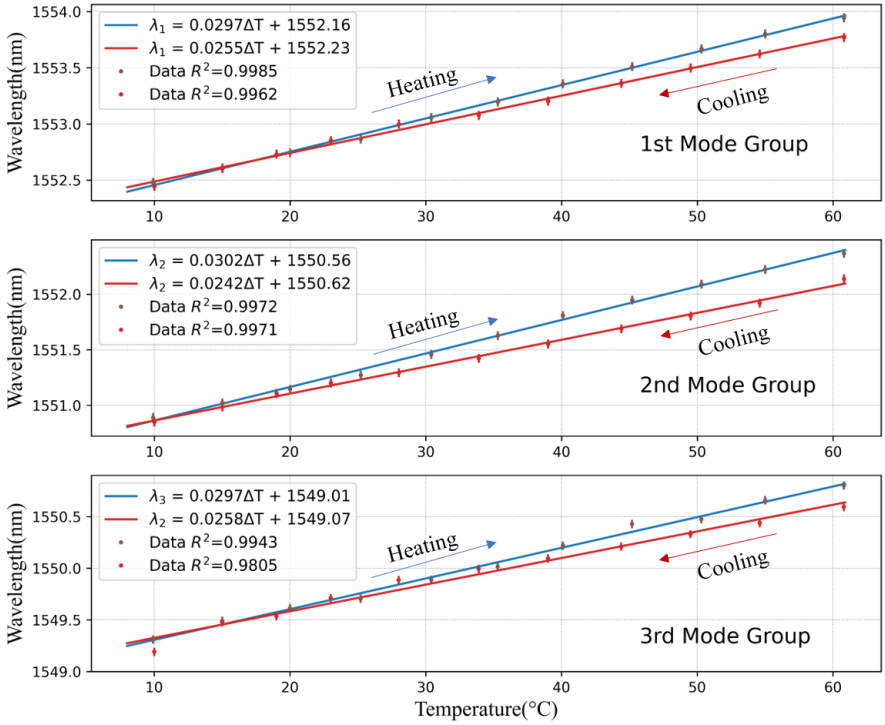

Fig. 10. Temperature response of different mode groups of grating #6 in CYTOP.

110 µW grating in CYTOP. It includes three mode groups: the first mode group (λ_1), the second mode group (λ_2), and the third mode group (λ_3). The linear fit on the points of Fig. 10 in the temperature range 10 °C to 60 °C is also displayed on the figure, and the numerical results are summarized in Table 2.

It is clearly seen that (1) all modes evolve linearly with the temperature with a coefficient of determination R^2 always better than 0.98, (2) the temperature sensitivity is practically independent of the monitored mode group, (3) there is a small hysteresis, (4) the heating up temperature sensitivities of the different mode groups are nearly identical with a mean value of 29.9 pm/°C,

Table 2. Temperature sensitivity of the FBG in CYTOP.

Mode Group	Heating Process (pm/°C)	Cooling Process (pm/°C)
λ_1	29.7	25.5
λ_2	30.2	24.2
λ_3	29.7	25.8
mean	29.9	25.2

and (5) the cooling down temperature sensitivities of the different mode groups are nearly identical with a mean value of 25.2 pm/°C. The average temperature sensitivity is thus 27.5 pm/°C, which is approximately three times that of the silica FBGs (10.37 pm/°C) and comparable to the results of [20] as well as with the estimation of Eq. 9.

5. Conclusion

In this work, we demonstrate the inscription of highly reflective fiber Bragg gratings (FBGs) in CYTOP fibers without over-clad by using 400 nm femtosecond pulses and the phase mask technique. The beam power and the length of the gratings are the key parameters to obtain a highly reflective FBG. For 2 mm-long gratings, a reflectivity up to 92 % is achieved in only 10 seconds with an average beam power of 80 µW. The wavelength locations of the FBG peaks due to the multimode behavior of the CYTOP fiber were numerically computed, and are in good agreement with the experimental ones. The mode-selective ability of the FBG comes from the coupling conditions of the SMF-CYTOP structure, and is important to interpret the experimental spectra.

The fabricated FBGs were designed to operate at 1550 nm to be compatible with existing silica-based FBGs and to use off-the-shelf classical measuring equipment available for the third telecommunication window. Nevertheless, making CYTOP fiber gratings in the low loss region (1000 nm to 1100 nm) of the polymer fiber only requires to change the phase mask, so the same writing efficiency will occur.

Finally, the temperature sensitivity of the different mode groups of the CYTOP-FBGs were measured with two temperature cycles consisting of consecutive heating up and cooling down processes. It is found that the sensitivity does not depend on the mode group under investigation, with a value around 29.9 pm/°C for the heating up and 25.2 pm/°C for the cooling down. The mean temperature sensitivity 27.5 pm/°C is therefore three times higher than that of silica FBGs (10.37 pm/°C).

Acknowledgments

This research is supported by the Fonds de la Recherche Scientifique - FNRS (T.0163.19 "RADPOF").

Disclosures

The authors declare no conflicts of interest.

References

1. C. Broadway, D. Kinet, A. Theodosiou, K. Kalli, A. Gusarov, C. Caucheteur, and P. Mégret, "CYTOP fibre Bragg grating sensors for harsh radiation environments," Sensors **19**, 2853 (2019).

2. X. Hu, D. Saez-Rodriguez, C. Marques, O. Bang, D. J. Webb, P. Mégret, and C. Caucheteur, "Polarization effects in polymer FBGs: study and use for transverse force sensing," Opt. Express **23**, 4581 (2015).
3. M. Lobry, M. Loyez, E. M. Hassan, K. Chah, M. C. DeRosa, E. Goormaghtigh, R. Wattiez, and C. Caucheteur, "Multimodal plasmonic optical fiber grating aptasensor," Opt. Express **28**, 7539 (2020).
4. X. Hu, P. Mégret, and C. Caucheteur, "Surface plasmon excitation at near-infrared wavelengths in polymer optical fibers," Opt. Lett. **40**, 3998 (2015).
5. X. Hu, C.-F. J. Pun, H.-Y. Tam, P. Mégret, and C. Caucheteur, "Highly reflective Bragg gratings in slightly etched step-index polymer optical fiber," Opt. Express **22**, 18807 (2014).
6. R. Min, B. Ortega, and C. Marques, "Fabrication of tunable chirped mPOF Bragg gratings using a uniform phase mask," Opt. Express **26**, 4411 (2018).
7. R. Min, S. Korganbayev, C. Molardi, C. Broadway, X. Hu, C. Caucheteur, O. Bang, P. Antunes, D. Tosi, C. Marques, and B. Ortega, "Largely tunable dispersion chirped polymer FBG," Opt. Lett. **43**, 5106 (2018).
8. B. G. Shin, J. H. Park, and J. J. Kim, "Low-loss, high-bandwidth graded-index plastic optical fiber fabricated by the centrifugal deposition method," Appl. Phys. Lett. p. 4645 (2003).
9. X. Hu, D. Kinet, K. Chah, C.-F. J. Pun, H.-Y. Tam, and C. Caucheteur, "Bragg grating inscription in PMMA optical fibers using 400-nm femtosecond pulses," Opt. Lett. **42**, 2794 (2017).
10. D. Vilarinho, A. Theodosiou, M. F. Domingues, P. Antunes, K. Kalli, P. André, and C. A. F. Marques, "Foot plantar pressure monitoring with CYTOP Bragg gratings sensing system," in *Proceedings of the 11th International Joint Conference on Biomedical Engineering Systems and Technologies,* (SCITEPRESS - Science and Technology Publications, 2018).
11. Y. Mizuno, T. Ma, R. Ishikawa, H. Lee, A. Theodosiou, K. Kalli, and K. Nakamura, "Twist dependencies of strain and temperature sensitivities of perfluorinated graded-index polymer optical fiber Bragg gratings," Appl. Phys. Express **12**, 082007 (2019).
12. A. Leal-Junior, A. Theodosiou, C. Díaz, C. Marques, M. Pontes, K. Kalli, and A. Frizera-Neto, "Polymer optical fiber Bragg gratings in CYTOP fibers for angle measurement with dynamic compensation," Polymers **10**, 674 (2018).
13. A. G. Leal-Junior, A. Theodosiou, R. Min, J. Casas, C. R. Diaz, W. M. D. Santos, M. J. Pontes, A. A. G. Siqueira, C. Marques, K. Kalli, and A. Frizera, "Quasi-distributed torque and displacement sensing on a series elastic actuator's spring using FBG arrays inscribed in CYTOP fibers," IEEE Sensors J. **19**, 4054–4061 (2019).
14. A. Theodosiou and K. Kalli, "Recent trends and advances of fibre Bragg grating sensors in CYTOP polymer optical fibres," Opt. Fiber Technol. **54**, 102079 (2020).
15. C. Broadway, R. Min, A. G. Leal-Junior, C. Marques, and C. Caucheteur, "Toward commercial polymer fiber Bragg grating sensors: Review and applications," J. Light. Technol. **37**, 2605–2615 (2019).
16. A. Theodosiou, A. Lacraz, A. Stassis, C. Koutsides, M. Komodromos, and K. Kalli, "Plane-by-plane femtosecond laser inscription method for single-peak Bragg gratings in multimode CYTOP polymer optical fiber," J. Light. Technol. p. 5404 (2017).
17. A. Ioannou, A. Theodosiou, C. Caucheteur, and K. Kalli, "Direct writing of plane-by-plane tilted fiber Bragg gratings using a femtosecond laser," Opt. Lett. **42**, 5198 (2017).
18. R. Min, B. Ortega, A. Leal-Junior, and C. Marques, "Fabrication and characterization of Bragg grating in CYTOP POF at 600-nm wavelength," IEEE Sensors Lett. p. 1 (2018).
19. M. Koerdt, S. Kibben, O. Bendig, S. Chandrashekhar, J. Hesselbach, C. Brauner, A. S. Herrmann, F. Vollertsen, and L. Kroll, "Fabrication and characterization of Bragg gratings in perfluorinated polymer optical fibers and their embedding in composites," Mechatronics. p. 137 (2016).
20. Y. Zheng, K. Bremer, and B. Roth, "Investigating the strain, temperature and humidity sensitivity of a multimode graded-index perfluorinated polymer optical fiber with Bragg grating," Sensors. p. 36 (2018).
21. *Information on the detail of CYTOP fiber <https://chromisfiber.com/products/gigapof-50sr/>*.
22. R. Min, B. Ortega, and C. Marques, "Fabrication of tunable chirped mPOF bragg gratings using a uniform phase mask," Opt. Express **26**, 4411 (2018).
23. R. Gravina, G. Testa, and R. Bernini, "Perfluorinated plastic optical fiber tapers for evanescent wave sensing," Sensors **9**, 10423–10433 (2009).
24. A. G. Mignani, R. Falciai, and L. Ciaccheri, "Evanescent wave absorption spectroscopy by means of bi-tapered multimode optical fibers," Appl. Spectrosc. **52**, 546–551 (1998).
25. J. Villatoro, D. Monzón-Hernández, and D. Luna-Moreno, "In-line optical fiber sensors based on cladded multimode tapered fibers," Appl. Opt. **43**, 5933 (2004).
26. F. Mitschke, *Fiber Optics* (Springer, 2016).
27. R. Olshansky, "Mode coupling effects in graded-index optical fibers," Appl. Opt. **14**, 935 (1975).
28. K. Kitayama, S. Seikai, and N. Uchida, "Impulse response prediction based on experimental mode coupling coefficient in a 10-km long graded-index fiber," IEEE J. Quantum Electron. **16**, 356–362 (1980).
29. A. Ghatak and K. Thyagarajan, *Introduction to fiber optics* (Cambridge University Press, 1998).
30. Y. Liu, J. Lit, X. Gu, and L. Wei, "Fiber comb filters based on UV-writing bragg gratings in graded-index multimode fibers," Opt. Express **13**, 8508 (2005).
31. A. Othonos, "Fiber Bragg gratings," Rev. Sci. Instruments **68**, 4309–4341 (1997).
32. W. W. Morey, G. Meltz, and W. H. Glenn, "Fiber optic bragg grating sensors," in *Fiber Optic and Laser Sensors VII,* R. P. DePaula and E. Udd, eds. (SPIE, 1990).

33. N. Safari Yazd, D. Kinet, C. Caucheteur, and P. Mégret, “Fiber Bragg grating characterization using factorial design,” Appl. Opt. **58**, 4898–4904 (2019).
34. A. Lacraz, M. Polis, A. Theodosiou, C. Koutsides, and K. Kalli, “Femtosecond laser inscribed Bragg gratings in low loss CYTOP polymer optical fiber,” IEEE Photonics Technol. Lett. p. 693 (2015).
35. *The information of SB 22 climate chamber <https://www.geminibv.com/labware/weiss-sb22-160140-climate-chamber/.*